ESKİŞEHİR TECHNICAL UNIVERSITY JOURNAL OF SCIENCE AND TECHNOLOGY
A- APPLIED SCIENCES AND ENGINEERING

2023, 24(4), pp. 300-308, DOI: 10.18038/estubtda.1330450

HARNESSING GOLD NANORODS FOR NON-ENZYMATIC GLUCOSE SENSING

Zeliha Cansu CANBEK OZDIL *

Department of Material Science and Nanotechnology Engineering, Faculty of Engineering, Yeditepe University, Istanbul, Turkey

ABSTRACT

This study presents a straightforward and non-enzymatic approach for glucose detection utilizing aggregated gold nanorods (GNRs) based on surface plasmon resonance (SPR). The GNRs exhibited enhanced sensitivity toward glucose concentrations of up to 10 mM. The LSPR-based glucose detection method demonstrated superior sensitivity, stability, ease of use, and a convenient readout. Moreover, the LSPR detection technique can be seamlessly integrated with various sensing platforms, offering the potential to expand the sensor's range and applicability. This study highlights the promising prospects of LSPR-based non-enzymatic glucose detection and its potential for integration into diverse sensing systems. For the 10 mM glucose solution, the addition of 5.85×10^9 GNRs caused a 136 nm shift. On the other hand, when 50 mM glucose is added, the shift amounted to 82 nm, while adding 100 mM glucose resulted in a shift of 71 nm. This implies that at lower glucose concentrations, the degree of aggregation is greater, suggesting a heightened sensitivity to smaller concentrations. TEM images depicted the formation of the gold nanorod aggregates upon the introduction of 10 mM glucose.

Keywords: Gold nanorods, Non-enzymatic glucose sensing, Nanosensor

1. INTRODUCTION

Low-cost, easy-to-use biosensors based on metal nanoparticles are proposed as new technology devices for the rapid detection of desired analytes providing high sensitivity and stability due to specific properties of metal nanoparticles called surface plasmon resonance (SPR) [1–3]. Namely, the optical response of nanoparticles, resulting from the collective oscillation of free conduction electrons in the metal surface under light irradiation at a resonance frequency, gives rise to SPR [4] in the light spectrum. The frequency of this oscillation is found generally in the visible region of UV-Vis spectra for materials like gold, silver, and copper. By changing the size of the nanoparticles, one can manipulate slightly the length of the plasmon peak to alter the optical properties of the material [5].

When isotropic nanoparticles are replaced with anisotropic analogs, optical features, and electrical and magnetic properties can be enhanced considerably with respect to previous cases due to their complex anisotropic structures. This kind of amelioration makes anisotropic nanoparticles quite desirable over isotropic ones for biosensing applications [6–8]. The single SPR splits into two different modes in the anisotropic nanoparticles; a transverse surface plasmon resonance (T-SPR), corresponding to the light absorption and scattering along the short axis of the particle, and a longitudinal surface plasmon resonance (L-SPR), corresponding to light absorption and scattering along the long axis of the particles. The L-SPR is quite dependent on the aspect ratio of the particle.

Such anisotropic nanoparticles can easily be tailored to enhance the capability of future MEMS (Micro-Electro-Mechanical Systems) devices [9], SERS (Surface Enhanced Raman Scattering) substrates [10], and state of art analyte sensing biosensors. The quality of the sensing is highly impacted by the variations in nanoparticle size, morphology, and the concentration of the nanoparticle [11]. To be able to use metal nanoparticles advantageously on any platform, we need to overcome some critical points such as:

*Corresponding Author: cansu.canbek@yeditepe.edu.tr
Received: 21.07.2023 Published: 27.12.2023

- Repeatability of the synthesis and high reproducibility of the same results should be attained, which is challenging for nano production.
- The synthesis should allow scalability for any real-life applications.
-

It should be noted that reproducibility is challenging for any nanomaterial production, considering that the production is highly dependent on reaction parameters [12].

There have been many studies on gold nanoparticle-based glucose sensors [3,13–17]. In the fabrication of such sensing platforms, the mechanism of sensing is based on the oxidation of target glucose to gluconolactone and producing hydrogen peroxide, which is a strong oxidizing agent, in the presence of glucose oxidase. The sensing is achieved indirectly by the etching activity of H_2O_2, released during the glucose oxidase enzymatic cycle, on the gold nanorods [13]. A schematic representation of the enzymatic glucose sensing mechanism is given in Figure 1a.

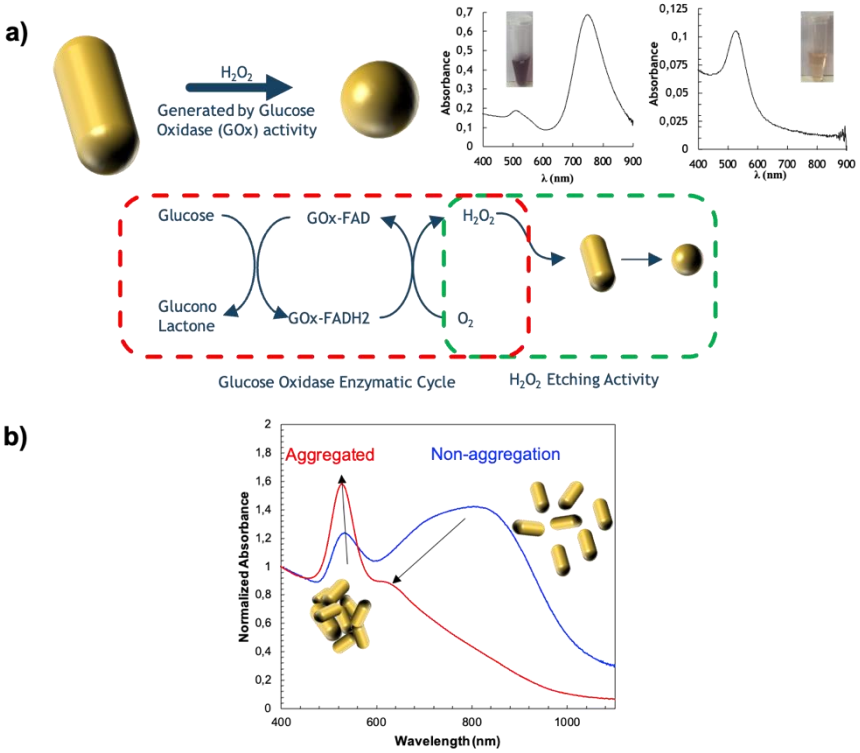

Figure 1. Schematic representation of a) enzymatic glucose sensing with GNRs based on etching via H_2O_2 activity b) non-enzymatic sensing with GNRs based on aggregation

There are limited studies unlocking the potential of gold nanorods for non-enzymatic glucose sensing since the material itself poses significant challenges [17,18]. In these works, agents like $Ag(NH_3)_2OH$, and dextran sulfate are introduced to induce aggregation to perform indirect sensing. While these tiny structures exhibit unique optical properties and demonstrate remarkable stability, their effective utilization in glucose-sensing applications demands overcoming several hurdles. One major obstacle is the need for sensitivity. Designing reliable and sensitive detection methods to translate the nanorod's optical responses into measurable signals necessitates sophisticated instrumentation and signal processing techniques.

In this work, we have provided a reproducible high-yield large-scale synthesis of gold nanorods via the chemical reduction method for non-enzymatic glucose sensing (Figure 1b). For the production of nanomaterials wet chemical synthesis method has been chosen due to the ease of the method and high reproducibility. Even though, the technique is largely affected by a number of factors (ionic strength of

water used during production, strict control of medium temperature, stirring efficiency, operator performing synthesis, etc.) [12], the fact that it does not require complex laboratory set-up and equipment brings many advantages. A schematic representation of the methodology used has been summarized in Figure 2.

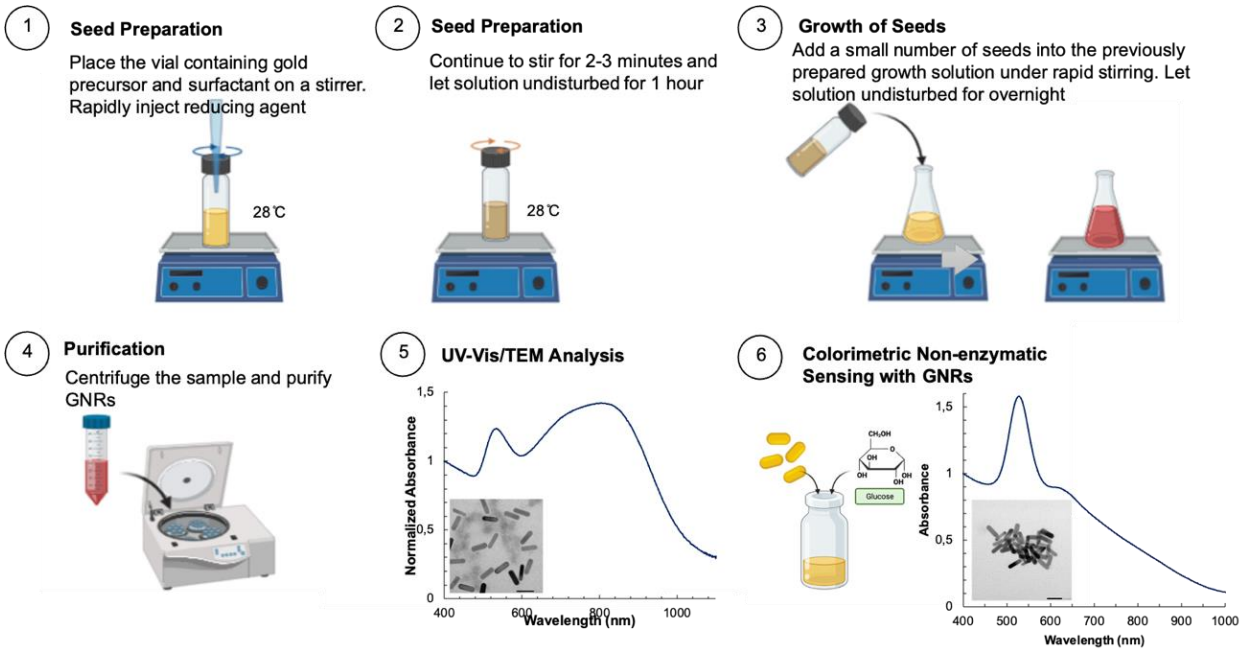

Figure 2. Schematic representation of the GNR production and characterization

2. MATERIALS and METHODS

2.1. Materials

Cetyltrimethylammonium bromide (CTAB, 99%), chloroauric acid ($HAuCl_4$, extra pure), silver nitrate ($AgNO_3$, extra pure), sodium borohydride ($NaBH_4$, 98%), and L-ascorbic acid were obtained from Sigma without further purification. All the glassware was cleaned with aqua regia and washed with distilled water before the experiments.

2.2. Synthesis of Seeds

The preparation of the seeds followed the procedure outlined in Nikoobakht and El-Sayed's study **[19]**. In this process, a rapid injection of 0.1 mL of an ice-cold 0.0264 M $NaBH_4$ solution is carried out into a mixture containing 0.025 mL of 0.05 M $HAuCl_4$ solution, and 4.7 mL of 0.1 M CTAB solution, at a temperature of 28 °C. Following the injection, the resulting mixture is stirred for a duration of 2 minutes and maintained at 28 °C for a minimum of 1 hour to allow excess $NaBH_4$ to evaporate. The light brown color of the mixture is indicative of the size of the seeds being smaller than 5 nm **[12]**.

2.3. Synthesis of Gold Nanorods

After the synthesis of seeds, the second step in production is their growth into final anisotropic shapes. In this stage, a reference growth solution with the following parameters has been prepared (Table 1).

Table 1 Chemical Parameters used during preparation of growth media

Stock Solution	Stock Solution Concentration	Added Quantity into Growth Solution (mL)	Final Concentration in Growth Solution [C_{final}] (mM)
$HAuCl_4 \bullet 3H_2O$	0.1 M	1.26	0.5
CTAB	0.1 M	250	100
$AgNO_3$	0.01 M	3.60	0.140
Ascorbic Acid	0.1 M	1.92	0.75
HCl	5 M	0.05	-

It should be well noted that a fresh stock solution of silver nitrate and ascorbic acid has been prepared for each synthesis for reproducibility. After the production of the growth solution, 1.5 mL of as-synthesized seed is injected rapidly into the growth media. The mixture is mixed over 20 seconds and kept at 28 °C without disturbance overnight to ensure that the growth is terminated.

2.4. Characterization of Gold Nanorods

UV-Vis spectroscopy experiments are realized by using Thermo Scientific NanoDrop 2000 Spectrophotometer. The UV-Vis spectrums of bare GNRs are recorded before any purification step. After recording, purification is performed by using a Beckman Culter Allegra centrifuge at 10000 g for 10 minutes in 3 steps. After each centrifugation, the supernatant is discarded and the sediment is washed with DI water to complete the volume to 10 mL.
Scanning electron microscopy (SEM) experiments are realized at Bogazici University Advanced Technologies R&D Centre Laboratory via Philips-FEI XL30 ESEM-FEG scanning Electron microscope at 30 kV. Transmission electron microscopy (TEM) observations are carried out by JEOL JEM 2100 Plus microscope equipped with Gatan US4000 CCD Camera operating at 200 kV. Before observation, samples are coated with plasma Au/Pd. Obtained images are analyzed via ImageJ software.

2.5. Non-enzymatic Glucose Sensing Experiments

To a series of 2 mL of freshly prepared and aerated glucose solutions, two different numbers of GNRs are added in scintillation vials. After 20 minutes waiting period, the samples are analyzed via UV-Vis spectroscopy.

3. RESULTS and DISCUSSION

The UV-Vis spectrum of GNRs, depicted in Figure 1, demonstrates two distinct peaks, one at 553 nm representing T-SPR and another at 804 nm representing L-SPR. The broad L-SPR peak can be attributed to the polydisperse nanorods. Via the UV-Vis spectrum, it is possible to characterize produced gold nanorods quantitatively. Mainly, the aspect ratio of as-produced gold nanorods can be deduced from simple relation with longitudinal surface plasmon band ($\lambda_{L\text{-}SPR}$) **[20]**:

$$AR = \frac{\lambda_{max} - 478}{96} \quad (1)$$

In our case, we estimated an AR of 3.39. Additionally, it is also possible to calculate the final colloidal gold concentration as 0.22 mM, converted from Au(I) into Au^0 (c_{Au}) via the following equation;

$$A_{400\,nm} = \varepsilon b c_{Au} \quad (2)$$

where A_{400nm} is the absorption band signal of gold at 400 nm, ε is the absorption coefficient ($2500 M^{-1}cm^{-1}$ ref) and b is the cell path length used during measurement (1 mm). The obtained values are summarized in Table 2.

Table 2 GNR solution parametric data

Symbol	Parameter	Numeric Value
l	Average length of GNR	45.81 nm
d	Average diameter of GNR	13.26 nm
r	Average radius of GNR	6.63 nm
AR	Aspect ratio (obtained by UV)	3.39
ρ	Density of Au atom	19.32 g/cm^{-3}
c_{Au}	Final Au(0) concentration	$2.2x10^{-4}$ mol/L
V_{total}	Total volume of GNR solution	256.85 mL
Mwt_{Au}	Molecular weight of gold	196.97 g/mol

After the deduction of the final gold concentration, it is possible to do a rough estimation of the number of GNRs by calculating the volume of a single nanorod via:

$$V_{single\ nanorod} = \pi r^2 l \tag{3}$$

where r is the diameter of the nanorod with an estimation of cylindrical shape for GNRs.

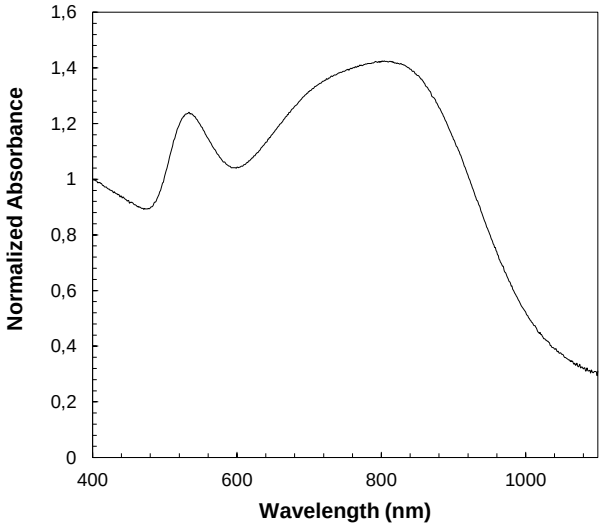

Figure 1. The UV-Vis spectrum of GNRs solution

The average radius and length of GNRs are obtained via SEM and TEM analysis. Corresponding SEM and TEM images are given in Figures 2a, b, and c. 50 particles are counted for the analysis. In microscopy images, GNRs appear more monodisperse in size and morphology. The discrepancy between the apparent polydispersity observed in the UV-Vis spectrum and the absence of such variability in microscopy images for GNRs can be attributed to the purification of the samples before microscopy observations. During the purification, by-products and excess CTAB, forming a thick organic layer around the nanorods and leading to a reduction in image resolution, are removed. This explains the difference between the UV-Vis spectrum and the microscopy images.

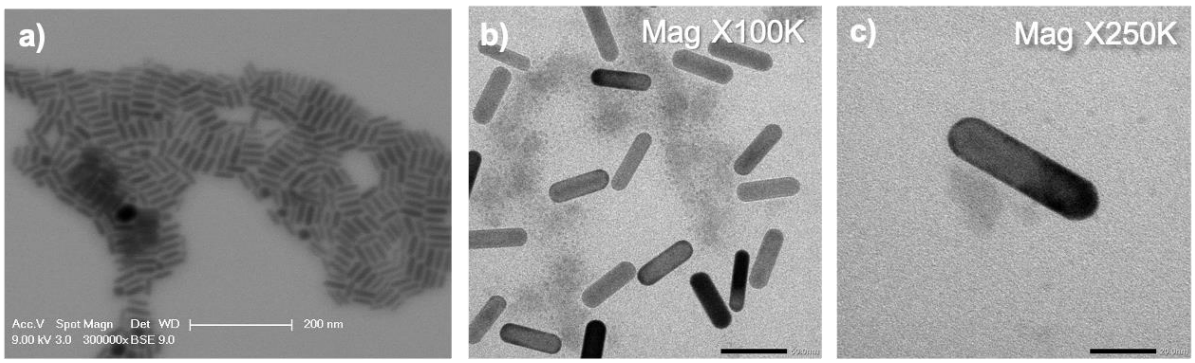

Figure 2. a) SEM micrograph of GNRs. TEM micrograph of b) GNRs and c) single GNR at higher magnification

Following that, the total mass of gold atoms in a single nanorod is calculated as 1.84 x10^{15}g via:

$$m_{Au} = pV_{single\ nanorod} \tag{4}$$

where *p* is the density of gold. From the mass it is possible to calculate the mole of gold atoms in a single gold nanorod (n_{Au}) by using the following equation:

$$n_{Au} = m_{Au}/Mwt_{Au} \tag{5}$$

where Mwt_{Au} is the molecular weight of gold. The total number of gold atoms in all gold nanorods (N_{Au}) would be calculated by multiplying the mole number of gold atoms in a single nanorod with the Avogadro number (N_a).

$$N_{Au} = N_a . n_{Au} \tag{6}$$

Finally, to calculate the total number of GNRs as 2.34x10^{11} in 1 mL solution, we have used the following equation:

$$Total\ number\ of\ Au\ nanorods = (c_{Au}.V_{total})/n_{Au} \tag{7}$$

L-SPR sensing experiments are conducted using three different concentrations of glucose (10 mM, 50 mM, and 200 mM) and two different numbers of GNRs (5.85x10^9 and 2.34x10^{10}). The number of GNRs is varied to investigate the impact of nanoparticle concentration on the L-SPR shift. With the addition of glucose, the L-SPR shows a blue shift, indicating a morphological transformation. In the case of the 10 mM glucose solution, the addition of 5.85x10^9 GNRs yielded a noticeable augmentation in the blue shift by 136 nm. Conversely, the introduction of 50 mM glucose elicited a shift of 82 nm, whereas the addition of 100 mM glucose resulted in a shift of 71 nm (Figure 3a). The observation of such a blue shift in the UV-Vis spectrum of GNRs upon the addition of glucose could be attributed to aggregation induced by polar glucose molecules. The hydroxyl groups (-OH) of glucose can interact with the positively charged CTAB molecules on the surface of the nanorods causing a blue shift in the L-SPR wavelength due to large aggregates. The aggregation after the addition of glucose is also visible in the corresponding TEM image depicted in Figure 3b.

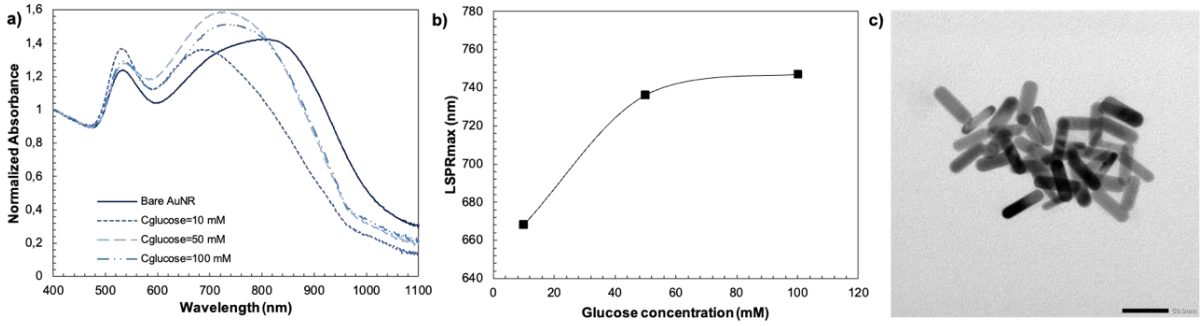

Figure 3. a) UV-Vis Spectrums of bare GNRs and Glucose-GNR mixtures with 10 mM, 50 mM, and 100 mM glucose concentrations and 5.85x109 number of GNRs c) Variation in L-SPR wavelength as an effect of change in glucose concentration b) Corresponding TEM image of the sample prepared with 10 mM glucose

A similar blue shift trend is observed when the number of GNRs is increased to $2.34x10^{10}$. However, apart from a blue shift in L-SPR, a significant decrease in the intensity of the L-SPR leads to a disappearance, suggesting that the GNRs are undergoing morphological reshaping towards isotropic shapes (Figure 4). When the concentration of GNRs is increased while keeping the amount of glucose constant in comparison to the previous case, the nanoparticles are more likely to come into close proximity and form aggregates. Such aggregation can lead to the coupling of plasmon modes in adjacent nanorods, resulting in a broadening and eventual disappearance of distinct L-SPR peaks. The interaction between the nanorods modifies their plasmonic behaviours, leading to a loss of well-defined resonance peaks.

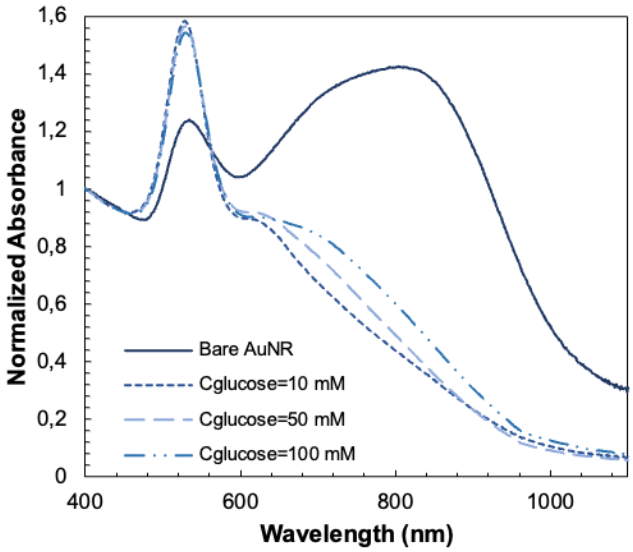

Figure 4. UV-Vis Spectrums of bare GNRs and Glucose-GNR mixtures with 10 mM, 50 mM, and 100 mM glucose concentrations and 2.34x1010 number of GNRs.

4. CONCLUSION

In conclusion, this study demonstrates a straightforward and non-enzymatic approach for LSPR-based glucose detection by using GNR aggregates, which exhibited heightened sensitivity towards a glucose concentration upto10 mM. Sensitivity below 10 mM can be further improved by employing nanorods with higher aspect ratios. With its superior sensitivity, stability, ease of use, and convenient readout, L-SPR detection can be combined with different types of sensing platforms to expand the sensor's range even further.

ACKNOWLEDGEMENTS

Financial support for this study was provided by Bogazici University BAP Funding under grant number 19A01P1. I would also like to express my gratitude to Elif Sumeyye Cirit for her assistance during sensing experiments.

CONFLICT OF INTEREST

The author stated that there are no conflicts of interest regarding the publication of this article.

REFERENCES

[1] Cao J, Sun T, Kenneth T, Grattan V. Development of gold nanorod-based localized surface plasmon resonance optical fiber biosensor. 22nd International Conference on Optical Fiber Sensors, 2012; p 8421.

[2] Saeed AA, Sánchez JLA, O'Sullivan CK, Abbas MN. DNA biosensors based on gold nanoparticles-modified graphene oxide for the detection of breast cancer biomarkers for early diagnosis. Bioelectrochemistry. 2017; 118, 91-99.

[3] Xu M, Song Y, Ye Y, et al. A novel flexible electrochemical glucose sensor based on gold nanoparticles/polyaniline arrays/carbon cloth electrode. Sensors and Actuators B: Chemical. 2017; 252, 1187-1193.

[4] Hu M, Chen J, Li ZY, et al. Gold nanostructures: engineering their plasmonic properties for biomedical applications. Chem Soc Rev. 2006; 35 (11), 1084-1094.

[5] Kelly KL, Coronado E, Zhao LL, Schatz GC. The Optical Properties of Metal Nanoparticles: The Influence of Size, Shape, and Dielectric Environment. J Phys Chem B. 2002; 107 (3), 668-677.

[6] Lohse SE, Murphy CJ. The Quest for Shape Control: A History of Gold Nanorod Synthesis. Chem Mater. 2013; 25(8), 1250-1261.

[7] Huang X, Neretina S, El-Sayed MA. Gold Nanorods: From Synthesis and Properties to Biological and Biomedical Applications. Advanced Materials. 2009; 21 (48), 4880-4910.

[8] Elechiguerra JL, Reyes-Gasga J, Yacaman MJ. The role of twinning in shape evolution of anisotropic noble metal nanostructures. J Mater Chem. 2006; 16 (40), 3906-3919.

[9] Ramadoss R. MEMS devices for biomedical applications. Solid State Technology. Published online 2013. https://electroiq.com/2013/10/mems-devices-for-biomedical-applications/.

[10] Scarabelli L, Coronado-Puchau M, Giner-Casares JJ, Langer J, Liz-Marzán LM. Monodisperse Gold Nanotriangles: Size Control, Large-Scale Self-Assembly, and Performance in Surface-Enhanced Raman Scattering. ACS Nano. 2014; 8, p 5833.

[11] Jana NR. Nanorod Shape Separation Using Surfactant Assisted Self-Assembly. Chem Commun. 2003;15, p 1950.

[12] Scarabelli L, Sánchez-Iglesias A, Pérez-Juste J, Liz-Marzán LM. A "Tips and Tricks" Practical Guide to the Synthesis of Gold Nanorods. J Phys Chem Lett. 2015; 6 (21), 4270-4279.

[13] Lin Y, Zhao M, Guo Y, et al. Multicolor Colormetric Biosensor for the Determination of Glucose based on the Etching of Gold Nanorods. Scientific Reports. 2016; 6 (1), p 37879.

[14] Chen KC, Li YL, Wu CW, Chiang CC. Glucose Sensor Using U-Shaped Optical Fiber Probe with Gold Nanoparticles and Glucose Oxidase. Sensors (Basel). 2018; 18 (4), p 1217.

[15] Yin B, Zheng W, Dong M, et al. An enzyme-mediated competitive colorimetric sensor based on Au@Ag bimetallic nanoparticles for highly sensitive detection of disease biomarkers. Analyst. 2017; 142 (16), 2954-2960.

[16] Tao Y, Luo F, Lin Y, Dong N, Li C, Lin Z. Quantitative gold nanorods based photothermal biosensor for glucose using a thermometer as readout. Talanta. 2021; 230, p 122364.

[17] Peng CA, Pachpinde S. Longitudinal Plasmonic Detection of Glucose Using Gold Nanorods. Nanomaterials and Nanotechnology. 2014; 4, p 9.

[18] Xianyu Y, Sun J, Li Y, Tian Y, Wang Z, Jiang X. An ultrasensitive, non-enzymatic glucose assay via gold nanorod-assisted generation of silver nanoparticles. Nanoscale. 2013; 5 (14): 6303-6306.

[19] Nikoobakht B, El-Sayed MA. Preparation and Growth Mechanism of Gold Nanorods (NRs) Using Seed-Mediated Growth Method. Chem Mater. 2003; 15, p 1957.

[20] Brioude A, Jiang XC, Pileni MP. Optical Properties of Gold Nanorods: DDA Simulations Supported by Experiments. J Phys Chem B. 2005; 109(27), 13138-13142.